Supporting Information

Spatially Modulated Stiffness on Hydrogel for Soft and Stretchable Integrated Electronics

Hao Liu[1,2], Moxiao Li[2,3], Shaobao Liu[4,5], Pengpeng Jia[1,2], Xiaojin Guo[2,6], Shangsheng Feng[2,3], Tian Jian Lu[4,5], Huayuan Yang[7], Fei Li[1,2#], Feng Xu[1,2#]

[1] *The Key Laboratory of Biomedical Information Engineering of Ministry of Education, School of Life Science and Technology, Xi'an Jiaotong University, Xi'an 710049, P.R. China*

[2] *Bioinspired Engineering and Biomechanics Center (BEBC), Xi'an Jiaotong University, Xi'an 710049, P.R. China*

[3] *State Key Laboratory for Strength and Vibration of Mechanical Structures, Aerospace School, Xi'an Jiaotong University, Xi'an 710049, P.R. China*

[4] *State Key Laboratory of Mechanics and Control of Mechanical Structures, Nanjing University of Aeronautics and Astronautics, Nanjing 210016, P.R. China*

[5] *Nanjing Center for Multifunctional Lightweight Materials and Structures (MLMS), Nanjing University of Aeronautics and Astronautics, Nanjing 210016, P.R. China*

[6] *School of Science, Xi'an Jiaotong University, Xi'an 710049,*

[7] *Department of Traditional Chinese Medicine Engineering, Shanghai University of Traditional Chinese Medicine, Shanghai 201203, P.R. China*

[#] *Corresponding authors: feili@mail.xjtu.edu.cn; fengxu@mail.xjtu.edu.cn*

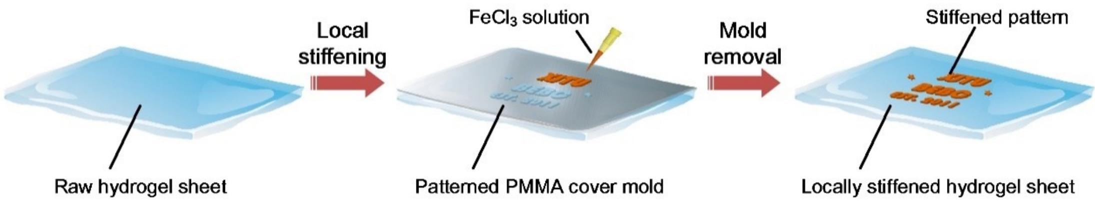

Figure S1. Schematic of fabrication process of the locally stiffened hydrogel. Local stiffening of hydrogel was achieved by covering a patterned polymethyl methacrylate (PMMA) board on the surface of hydrogel and then adding $FeCl_3$ solution to the hollow, patterned area.

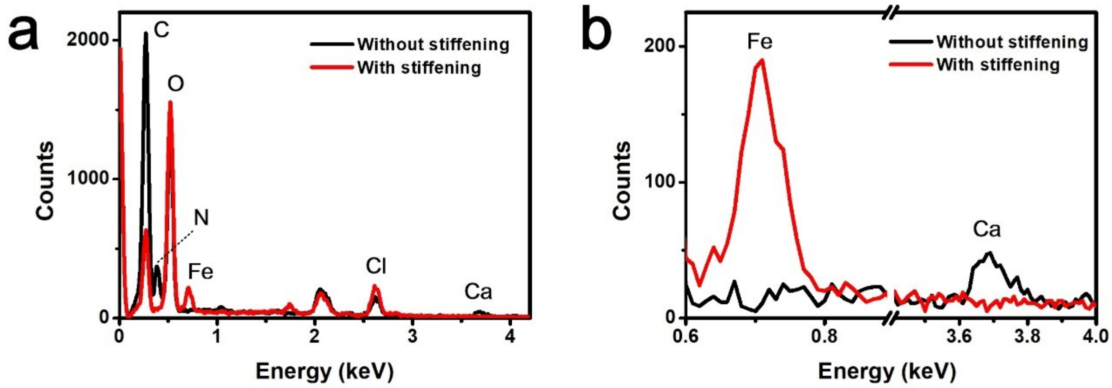

Figure S2. Energy X-ray dispersive spectroscopy result on element composition of the hydrogel with and without stiffening treatment: full spectrum (a) and zoom-in spectrum (b).

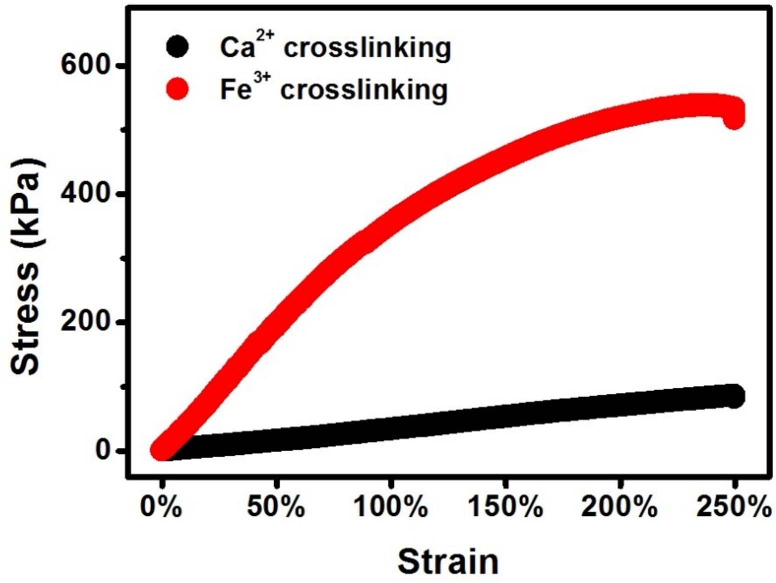

Figure S3. Stress-strain curves of PAAm-alginate hydrogels crosslinking with Ca^{2+} and Fe^{3+}.

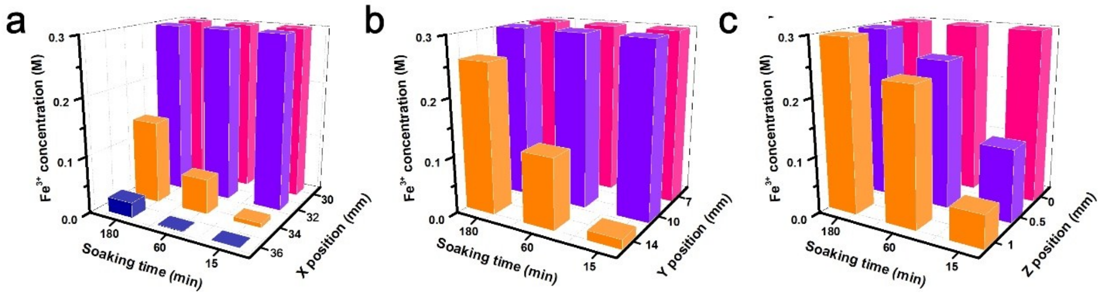

Figure S4. Fe^{3+} concentration as a function of $FeCl_3$ solution soaking time and position to depict diffusion of Fe^{3+}in hydrogel along x (a), y (b) and z (c) axes.

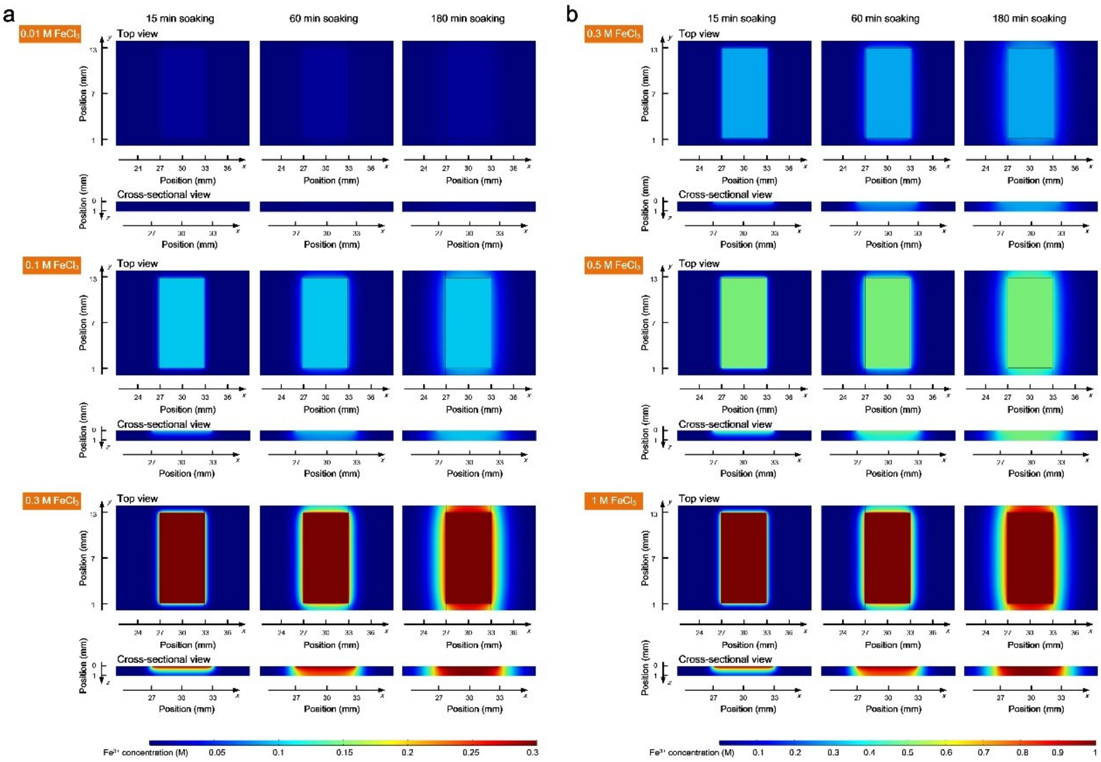

Figure S5. FEA simulation results of Fe^{3+} concentration distribution in hydrogel when soaked in $FeCl_3$ solution of different concentrations (0.01, 0.1, 0.3, 0.5 and 1 M) for different periods of time (15, 60 and 180 min).

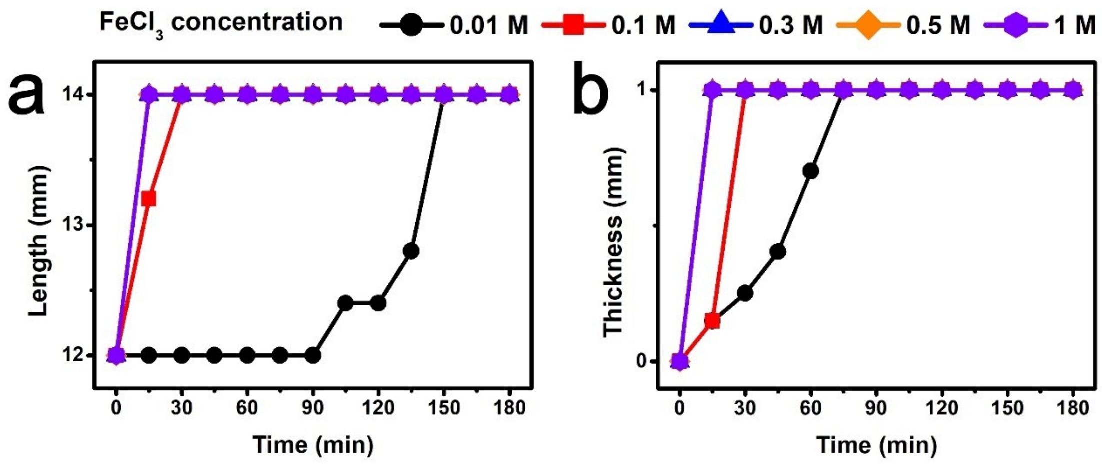

Figure S6. Simulation results on length (a) and thickness (b) of the stiffened pattern as a function of time treated with FeCl3 solution of different concentrations.

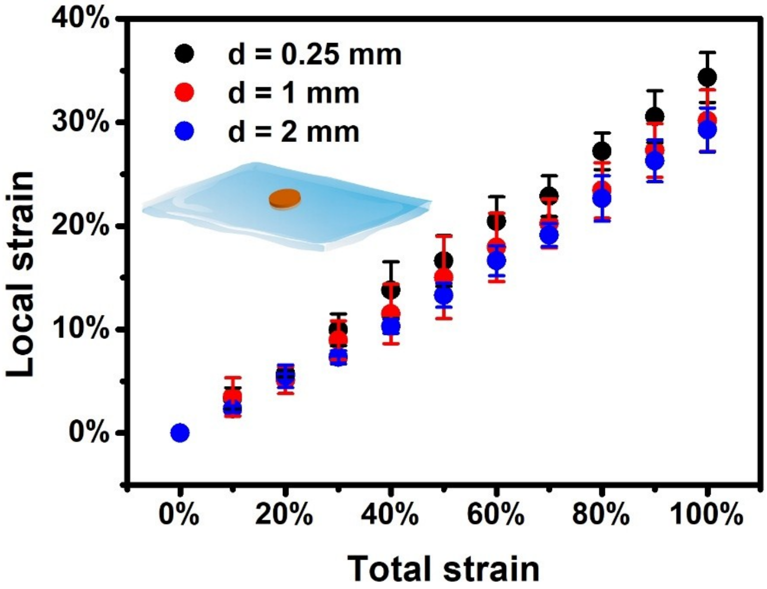

Figure S7. The strain shielding effect of the locally stiffened hydrogel with different pattern sizes (diameters of 0.25, 1 and 2 mm for a circle pattern).

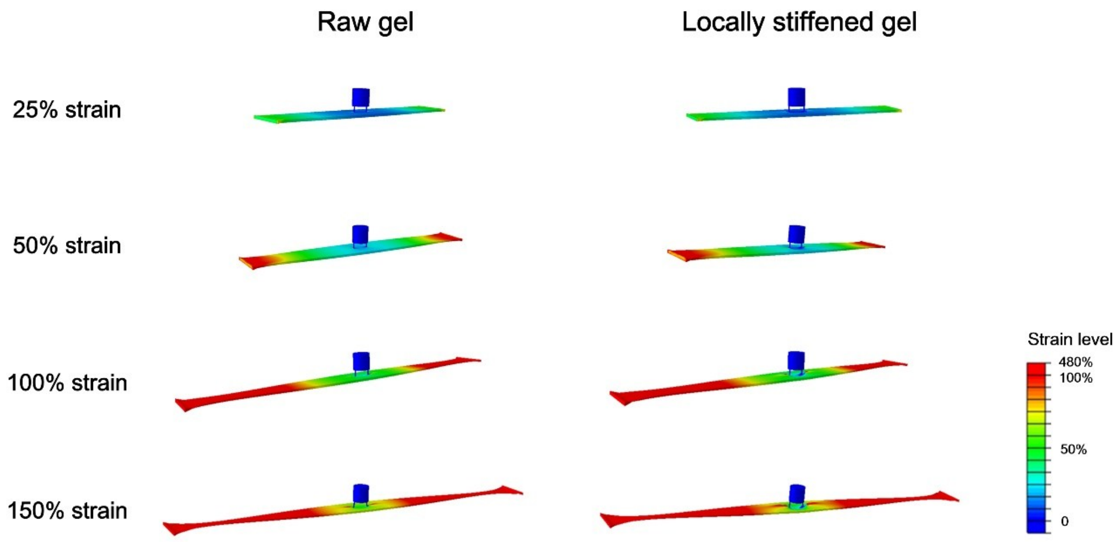

Figure S8. Finite element analysis results of strain distribution on hydrogel under different strain levels.

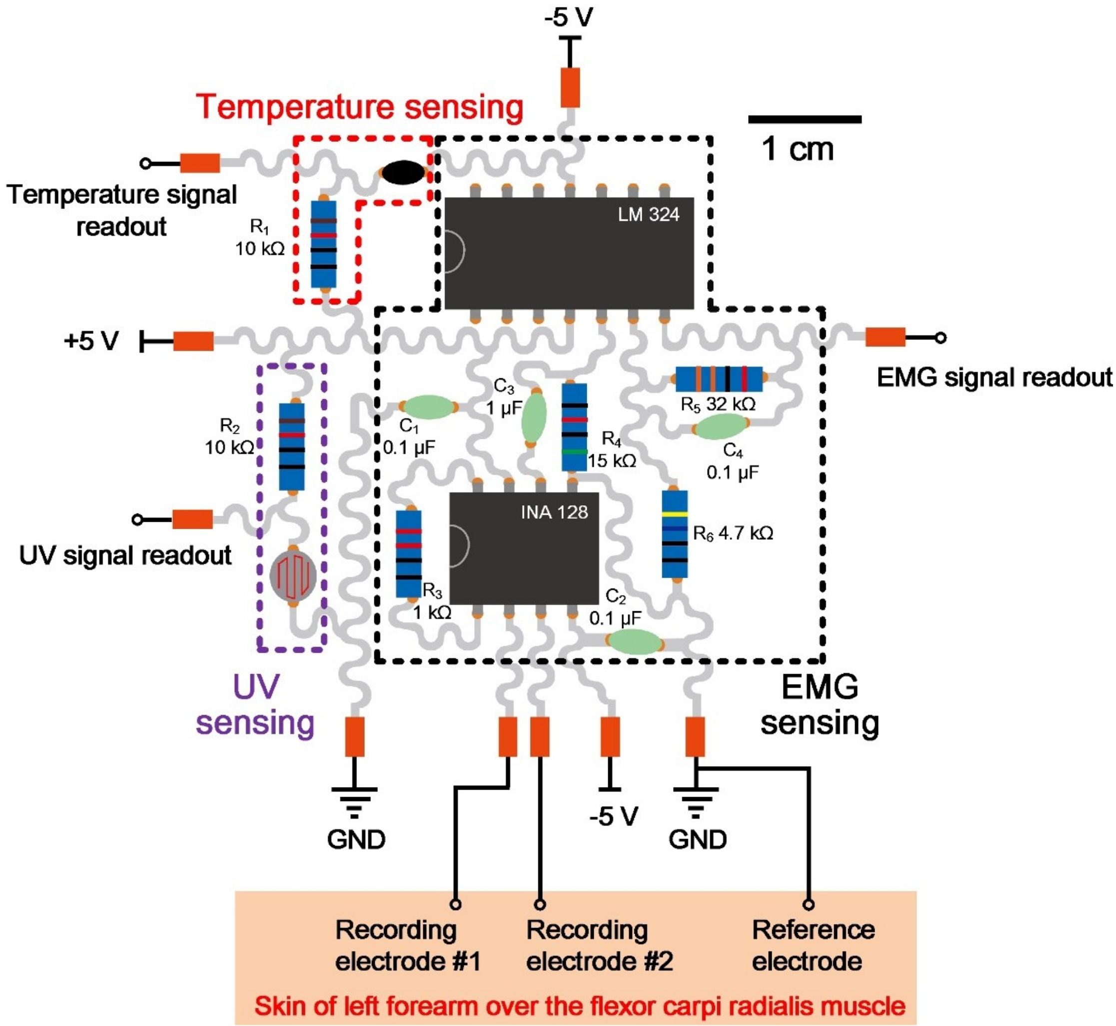

Figure S9. Schematic illustration of circuit design and component selection of the multifunctional hydrogel electronic device. The temperature sensing module consists of a thermistor and a fixed resistor (R_1). The UV sensing module consists of a photoresistor and a fixed resistor (R_2). The EMG sensing module consists of an instrumentation amplifier chip (INA 128), an operational amplifier chip (LM 324), and several fixed resistors (R_3, R_4, R_5 and R_6) and capacitors (C_1, C_2, C_3 and C_4). Among them, R_4 and C_3 constitute the high pass filtering unit, and R_5 and C_4 constitute the low pass filtering unit. Copper tapes work as electrodes to connect the sensing circuit with power supply, signal detection and data readout.

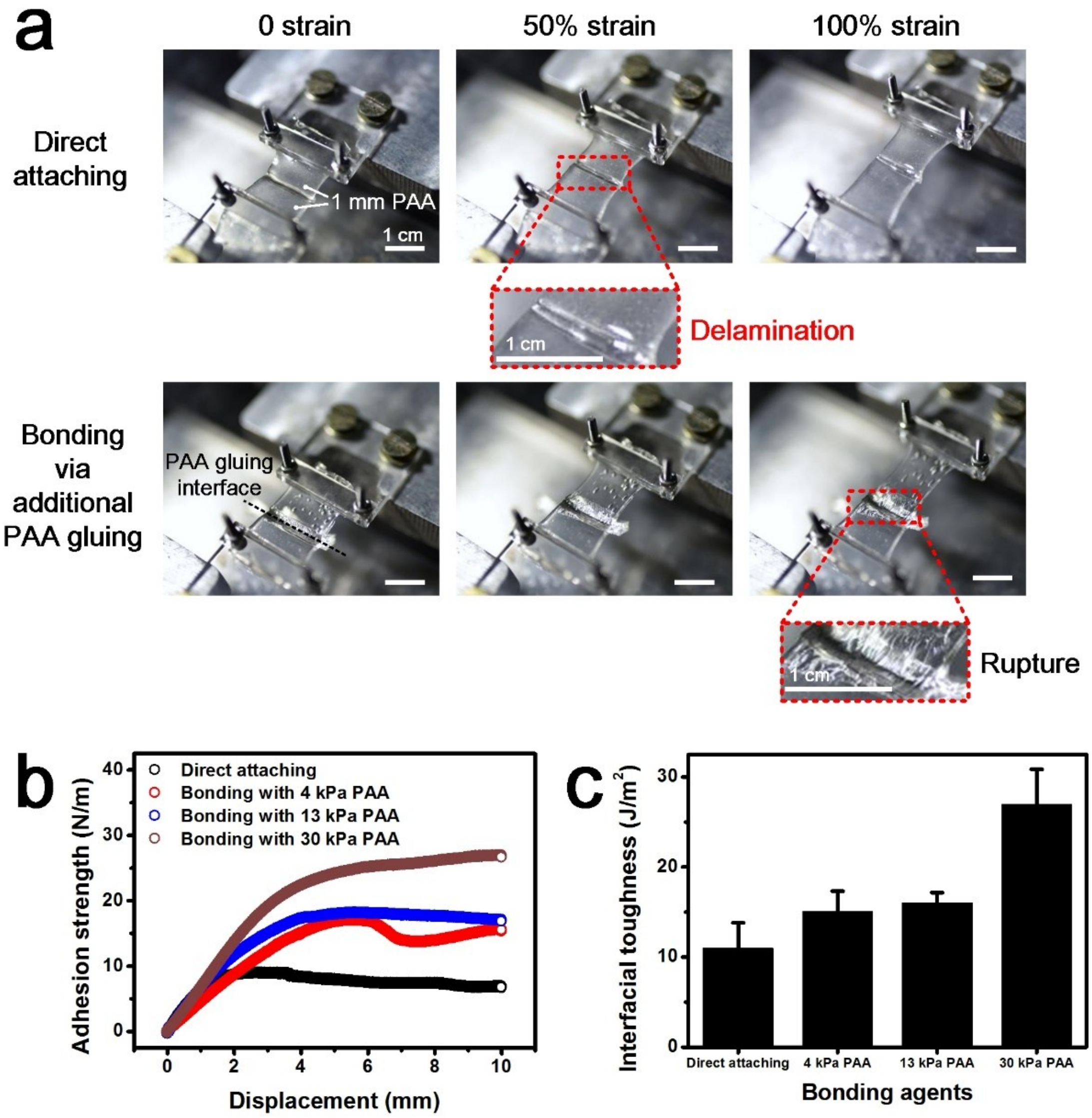

Figure S10. Tough bonding of PAAm hydrogels through additional PAAm gluing. (a) T-shape peeling test results show that delamination can be clearly observed when two PAAm layers are simply attached to each other, while additionally coating with PAAm precursor solution between the two hydrogel layers forms tough bonding to sustain larger strains. (b, c) Adhesion strength (b) and interfacial toughness (c) of the PAAm-PAAm bonded system using different bonding agents. Error bars represent standard deviation ($N = 5$).

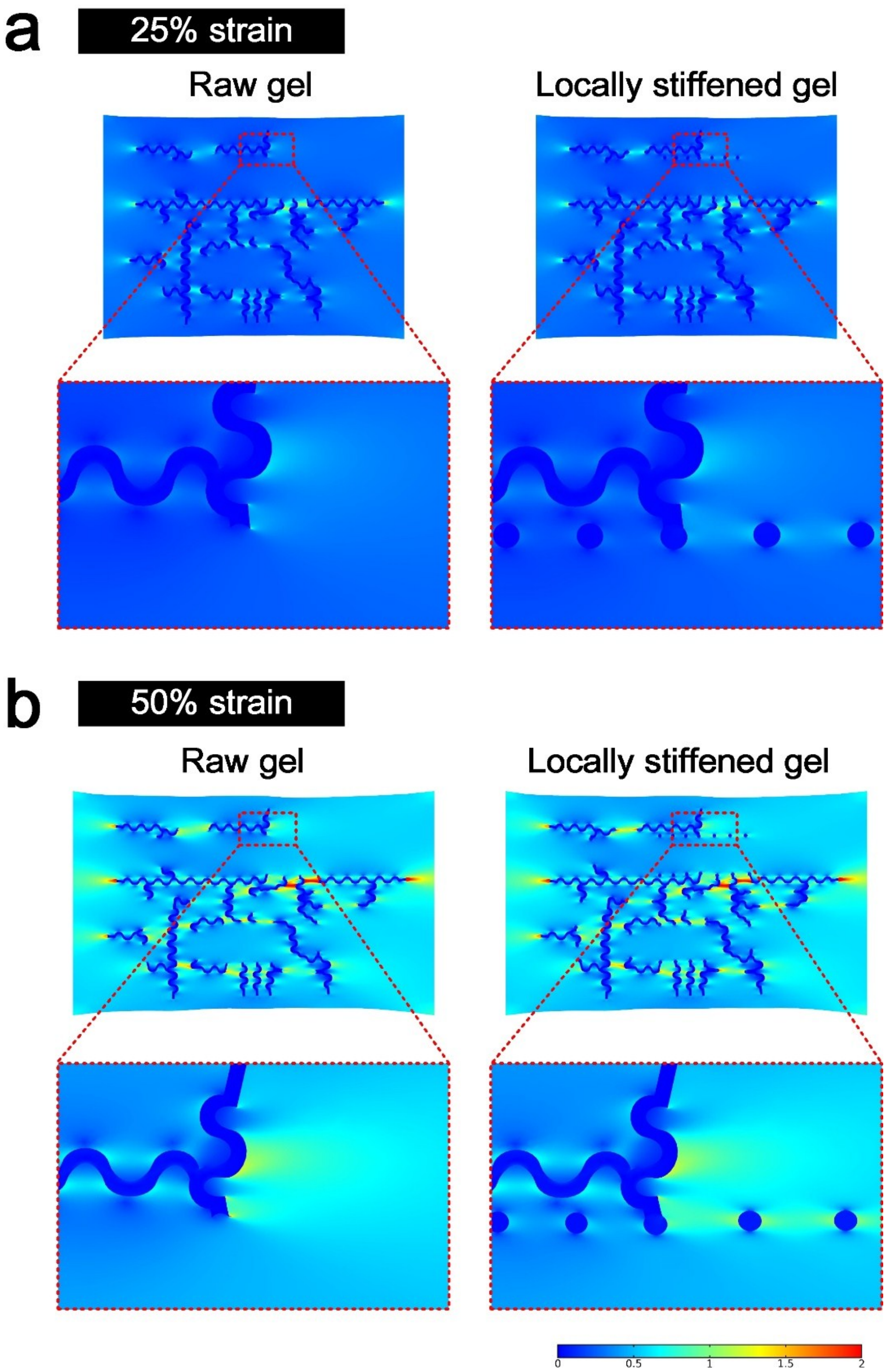

Figure S11. Finite element analysis results of strain distribution on a raw hydrogel substrate and a locally stiffened hydrogel substrate for the wearable, multifunctional electronic device under strain levels of (a) 25% and (b) 50%.

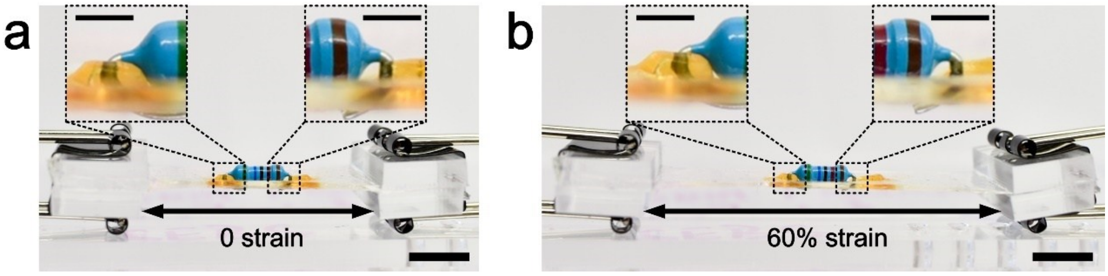

Figure S12. Digital photos of a resistor-integrated hydrogel electronic device before (a) and after (b) stretch to 60% strain. Scale bars represent 1 cm. Insets: enlarged pictures of pins of the resistor. Scale bars represent 2 mm.

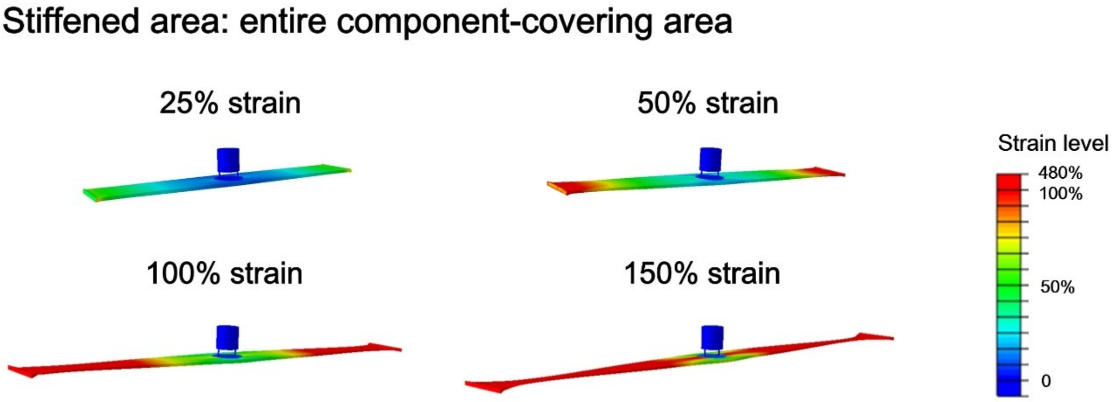

Figure S13. Finite element analysis results of strain distribution on hydrogel under different strain levels. For integration with surface-mounted components, the entire component-covering area on hydrogel is stiffened in this case.

Table S1. Preparation protocol for corresponding precursor solutions (1 mL) of PAAm-alginate hydrogel with different mechanical properties

	Deionized water	Acrylamide 50 wt%	MBA 1.25 wt%	APS 10 wt%	TEMED
4 kPa PAAm	821	120	48	10	1
13 kPa PAAm	565	400	24	10	1
30 kPa PAAm	549	200	240	10	1

All units in the table are μL.